OncoTargets and Therapy

Dovepress
Taylor & Francis Group

Open Access Full Text Article

ORIGINAL RESEARCH

A Pyroptosis-Related LncRNA Signature for Predicting Prognosis, Immune Features and Drug Sensitivity in Ovarian Cancer

Po-Wu Liu[1,2,*], Zhao-Yi Liu[2,*], Shi-Jia Deng[2,*], Xiu Zhang[2], Zhi-Bin Wang[2], Na-Yiyuan Wu[2], Chao-Shui Liu[3], Ming-Hua Hu[3], Jing Wang[2], He Li[2,3]

[1]University of South China, Hengyang Medical School, Graduate Collaborative Training Base of Hunan Cancer Hospital, Hengyang, Hunan, 421001, People's Republic of China; [2]Hunan Clinical Research Center in Gynecologic Cancer, The Affiliated Cancer Hospital of Xiangya School of Medicine, Central South University/Hunan Cancer Hospital, Changsha, Hunan, 410013, People's Republic of China; [3]Hunan Provincial Key Laboratory of the Research and Development of Novel Pharmaceutical Preparations, Changsha Medical University, Changsha, Hunan, 410219, People's Republic of China

*These authors contributed equally to this work

Correspondence: Jing Wang; He Li, Email wangjing0081@hnca.org.cn; lihe@hnca.org.cn

Background: Multiple studies have suggested that lncRNAs and pyroptosis play important roles in ovarian cancer (OC). However, the function of pyroptosis-related lncRNAs (PRLs) in OC is not fully understood.

Methods: Clinical information and RNA-seq data of OC patients (n = 379) were collected from TCGA database. Pearson correlation analysis and univariate Cox analysis were performed to identify prognostic PRLs, respectively. LASSO-COX regression was utilized to construct a prognostic PRLs signature. Kaplan–Meier (K–M) curve analyses and receiver operating characteristics (ROC) were used to evaluate the prognostic prediction of the signature. The association between risk score and tumor microenvironment infiltration, immunotherapy response and chemotherapy sensitivity were also analyzed. In addition, the function of TYMSOS on OC and pyroptosis was experimentally confirmed in cell lines.

Results: Firstly, 32 prognostic PRLs were identified, and a novel prognostic PRLs signature was constructed and validated. Surprisingly, the prognostic PRLs signature could solidly predict the clinical outcome of patients with OC and patients with high-risk score shown a short overall survival. GSEA results suggested that the RPLs were mainly enriched in the inflammatory response pathway, p53 pathway, TGF-β signaling and TNFα signaling. Besides, our results demonstrated that the risk score was significantly associated with patients with immune infiltration, immunotherapy response and the sensitivity of veliparib and metformin. Furthermore, the oncogene effect of TYMSOS on OC by inhibiting pyroptosis was verified by experiments.

Conclusion: This study found that the prognostic PRLs signature may serve as an efficient biomarker in predicting the prognosis, tumor microenvironment infiltration, and sensitivity of chemotherapeutic agents. TYMSOS is a potential biomarker in OC, and it might promote tumor progression by inhibiting pyroptosis.

Keywords: pyroptosis, ovarian cancer, prognosis, immune microenvironment, signature

Introduction

Worldwide, ovarian cancer (OC) ranks as the third most common gynecologic cancer and patients with OC suffer from an extremely high recurrence and mortality rate.[1] In 2023, there were 19,710 new cases and 13,270 deaths of OC in the United States, and it was the sixth most prevalent cause of death among all women who died of cancer.[2] Due to the absence of early physical signs, over 70% of epithelial ovarian cancer (EOC) cases are reported to be newly diagnosed at advanced stages with a five-year survival rate of approximately 48%.[3] The standard of therapy for OC is tumor cytoreductive surgery in conjunction with platinum-based chemotherapy. However, most patients recur within two years. It indicates that recurrence and drug resistance are the major challenges that need to be addressed.[4] Given the

Received: 10 October 2024
Accepted: 16 April 2025
Published: 23 April 2025

limitations of current OC treatment, new targets for therapy are desired to enhance the clinical outcome of OC. In this context, there is an overwhelming urgency for robust prognostic models to render targeted therapies more plausible.

At present, multiple evidences have demonstrated that pyroptosis plays important roles in cancer.[5] Pyroptosis, which is morphologically characterized by swollen cell lysis, rupture of cell membranes and the release of cell contents, is a programmed cell death referring to the Gasdermin family-induced and caused by the inflammasome, and ultimately activating a cascade of enlarged inflammatory responses.[6–8] As is known to us, there are two main forms of pyroptosis: i) the caspase-1 dependent classical pathway; ii) the caspase-4/5/11 reliant non-classical pathway. In the non-classical inflammasome pathway, bacterial lipopolysaccharide (LPS) induces pyroptosis by initiating caspase-4/5/11 cleavage of gasdermin D (GSDMD). In the typical inflammasome pathway, the inflammasome recruits and combines with ASC (CARD-containing apoptosis-associated spot-like protein), resulting in ASC gathering, which in turn activates caspase-1. Caspase-1 is involved in the cleavage and maturation of pro-IL-18/1b and the cleavage of GSDMD. Subsequently, the excretion of IL-18/1b causes the influx of water, cell swelling and permeability lysis.[9–11] Recent findings demonstrated that pyroptosis played an emerging role in various diseases, including autoimmune and inflammatory diseases, infectious diseases, deafness, and cancer.[12–16] In cancer, it is suggested that the process of pyroptosis inhibits tumorigenesis and progression, conversely, it serves as a pro-inflammatory signal to establish a microenvironment suitable for tumor cell growth.[17–20] Yet, the exact function of pyroptosis was poorly investigated in OC.

Long non-coding RNAs (lncRNAs) are identified as a group of RNA molecules over 200 bp in length that are not translated into proteins. They are reported to participate in various biological processes, such as epigenetic modifications, inheritance stamping, chromatin organization, and protein amendment.[21] Several studies have indicated that lncRNAs might be engaged in OC and pyroptosis.[22–25] Previous studies have primarily focused on the utility of protein-coding genes of pyroptosis, lncRNAs related with pyroptosis (PRLs) have barely been reported in OC.[26–28] Therefore, the identification of PRLs is essential for deciphering the underlying motifs of pyroptosis in OC and investigating new therapeutic targets. In our study, PRLs were first screened by using the Pearson correlation analysis. Furthermore, a prognostic signature was constructed based on the PRLs. The prognostic PRLs signature significantly predicted the clinical outcome of OC patients in high-risk subgroup and low-risk subgroup with a high diagnostic accuracy. In addition, it was correlated with the tumor microenvironment infiltration, immunotherapy response and drug sensitivity. Finally, we validated the effects of TYMSOS on cell proliferation, invasion and migration in OC cell lines.

Materials and Methods

Data Acquisition and Preprocessing

In this study, TCGA dataset was publicly accessible and downloaded from the University of California, Santa Cruz (UCSC) Xena website (https://xena.ucsc.edu). A total of 379 OC patient samples were available from the TCGA-RNA-seq dataset, and 2 patients without prognostic information were excluded. Finally, only 377 patients were retained for subsequent analysis. The distribution of clinical information was presented in Table 1. Normal samples were acquired

Table 1 Clinical Characteristics of OC Subjects in TCGA-RNA-Seq Dataset (n = 377)

Characteristics	Training Cohort	Test Cohort	Sum Cohort	p-value*
Age				0.63
Younger (≤55y)	76	71	147	
Older (>55y)	113	117	230	
FIGO Stage				0.20
I	0	1	1	
II	9	14	23	
III	153	140	293	
IV	26	31	57	
NA	1	2	3	

(*Continued*)

Table 1 (Continued).

Characteristics	Training Cohort	Test Cohort	Sum Cohort	p-value*
Grade				0.13
G1	0	1	1	
G2	28	17	45	
G3	156	164	320	
G4	1	0	1	
GB	1	1	2	
GX	1	0	1	
NA	0	2	2	
Tumor residual				0.42
No Macroscopic disease	35	32	67	
1–10 mm	89	82	171	
11–20 mm	15	12	27	
>20 mm	29	41	70	
NA	21	21	42	
Lymphatic invasion				0.32
YES	53	48	101	
NO	21	27	48	
NA	115	113	228	
Subdivision				0.19
Left/ right	57	45	102	
Bilateral	123	132	255	
NA	9	11	20	
Chemotherapy				0.32
Yes	174	176	350	
Platinum-based	163	169	332	
Others	11	7	18	
NO	15	12	27	

Note: *Training cohort vs Test cohort.

from the GTEx dataset. E-MTAB-1814 dataset was downloaded from the ArrayExpress website (https://www.ebi.ac.uk/arrayexpress/). GSE26193 dataset was downloaded from GEO database (www.ncbi.nlm.nih.gov/geo/). The quality control and gene expression values were normalized by log2(X+1) transformation with R package "limma" and "reshape2". For the gene annotation, we transformed the Ensembl IDs to gene symbols and genes expression values with multiple probes are determined as the average of the individual probes. The whole TCGA data were randomly split into two equal cohorts: training cohort and test cohort, which was also applied to validate as a sum cohort. There was no difference in pathological features and treatment. The PRGs (pyroptosis-related genes) were obtained from the previously published literature and MSigDB dataset (www.gsea-msigdb.org/gsea/msigdb/).[22–29]

Identification of PRLs

The lncRNA annotation file was acquired from the GENCODE website for the annotation of lncRNAs. Consequently, 14826 lncRNAs were obtained from the TCGA-RNA-Seq cohort.[30] Pearson correlation analysis was used to screen PRLs. Those lncRNAs with $r > 0.4$ and $P < 0.001$ were considered as the PRLs.[31] To determine the prognostic value of PRLs, we further conducted univariate Cox regression analysis by using the "survival" package, and the hazard ratios (HR) with 95% confidence intervals (CIs) were examined. $P < 0.05$ indicated that PRLs were significantly associated with overall survival (OS) and considered as prognostic PRLs. PRLs with HR > 1 were considered to be risk factors, whereas those with HR < 1 were considered to be protective factors.

Construction of Prognostic PRLs Signature

A risk signature was constructed by performing the LASSO-COX regression on the prognostic-related lncRNAs using the "glmnet" package.[32] Through 1000 cross-validation, a panel of genes and their LASSO coefficients were obtained. The risk score for the signature was calculated using the following formula:

$$\text{Risk score} = \sum_{i=1}^{n} \beta_n x_n$$

(n, is the number of the gene; β, LASSO coefficient; X, the expression of each prognostic PRLs in each sample). Based on the best cutoff risk score determined by the "survcutpoint" function of the "survminer" R package, patients were divided into high-risk and low-risk subgroups. Kaplan–Meier method with the long-rank test was performed to reveal the difference of OS between the high- and low-risk subgroups by using the "survival" package. Besides, the time-dependent ROC curve and area under the curve (AUC) were applied to evaluate the prediction accuracy of the signature. All the time-dependent ROC curves were calculated by the "SurvivalROC" package and drawn by the "ggplot2" package.

Nomogram Construction Based on Clinical Features and Risk Score

Univariate and multivariate Cox regression were performed to select the prognostic risk factors. The nomogram model was constructed using the "RMS" package to predict the 3, 5-year survival probability. The calibration curves were used to assess the concordance of the observed and predicted rates of 3, 5-year overall survival.[33]

Estimation of Tumor-Infiltration, Immunotherapy and Drug Sensitivity

First, all microenvironment scores, including EstimateScore, ImmuneScore, PurityScore, and StromalScore were calculated using the ESTIMATE algorithm (https://bioinformatics.mdanderson.org/public-software/estimate/).[34] The infiltrating immune cells scores and the activity of immune-related pathways were calculated by performing the ssGSEA analysis with "gsva" package.[35] Tumor Immune Dysfunction and Exclusion (TIDE) algorithm (http://tide.dfci.harvard.edu/), which is commonly utilized to accurately predict the outcome of patients treated with immune checkpoint inhibitors (ICIs), was employed to evaluate the immunotherapy response.[36] The drug sensitivity of each patient was evaluated using the Genomics of Drug Sensitivity in Cancer database (GDSC, https://www.cancerrxgene.org). The half-maximal inhibitory concentration (IC50) of all drugs commonly used to treat tumors was calculated and represented by the drug sensitivity. The R package "pRRopheticRredic" was used with 10-fold cross-validation and other parameters by default.[37]

Functional Enrichment Analysis

Gene set enrichment analysis (GSEA) was performed to identify the potential molecular mechanisms or potential functional pathways associated with prognostic PRLs signature. It was performed in Java GSEA v. 4.0.3 on the Molecular Signatures Database (MSigDB). Kyoto Encyclopedia of Genes and Genomes (KEGG) dataset and Gene Ontology (GO) enrichment analyses were performed to identify enriched pathways between the high- and the low-risk subgroup by using the "clusterProfiler" R package. $|NES| > 1$ and false discovery rate (FDR) <0.05 were considered statistically significant.

Cell Culture

The human ovarian cancer cell lines A2780 and SKOV3 were purchased from China Center for Type Culture Collection (CCTCC, Wuhan, China) and both cultured in RPMI-1640 medium, supplemented with 10% fetal bovine serum (FBS) and 1% penicillin/streptomycin. They were cultured in a sterile incubator maintained at 37°C with 5% CO_2. The cells in logarithmic growth phase were collected for subsequent experiments.

RNA Extraction and Quantitative PCR

Total RNA was extracted using TRIZOL reagent according to the manufacturer's protocol (Invitrogen, 15596-026). Reverse transcription of cDNA was performed using the PrimeScript RT kit (Takara, RR047A, Japan). RT-qPCR assays

were performed using LightCycler480 detector (Roche, USA). The relative mRNA levels were calculated using the comparative Ct method with GAPDH as the reference gene. All the primers are listed in Supplement Table 1.

Colony Forming Assay

Cells were transfected with or without lncRNA-targeted siRNAs for about 48 h. Then, cells with the density of 200 cells/well were plated in the six-well culture plates and cultured for about 2 weeks. The cellular colonies were counted by staining with crystal violet.

Cell Counting Kit-8 Assay

Cell viability was measured by using Cell Counting Kit-8 (Proteintech, PF00004) after transfection with or without lncRNA targeted siRNAs for 24 h, 48 h, and 72 h, respectively. Briefly, cells were incubated with RPMI-1640 medium with 10% CCK-8 at 37°C. After 4 h incubation, the OD value was measured at 450nm.

Transwell Migration and Invasion

A total of $2*10^5$ cells were seeded in the upper chamber of transwell plates with serum-free medium and were then incubated for 48 hours. To perform invasion experiments, the upper chambers were covered with a mixture of RPMI-1640 and Matrigel. Finally, the cells at the lumen were removed with a cotton swab, whereas the cells across the membrane were stained with 0.5% crystal violet, observed and counted under 100x magnification.

Statistical Analysis

Significant quantitative differences between groups were analyzed using the two-tailed Students' *t*-test, whereas differences among groups were analyzed using the one-way ANOVA. Kaplan–Meier curves and Log rank test were used to calculate the overall survival rate. All statistical analyses were performed using R software (version 4.0.2). * means $P < 0.05$, ** means $P < 0.01$, *** means $P < 0.001$. $P < 0.05$ was considered statistically significant.

Results

Clinical Characteristics of the Study Patients

The mRNA and lncRNA expression profiles of 377 OC subjects were screened in the TCGA-RNA-seq dataset. All patients were randomly separated into training cohort (n = 189) and test cohort (n = 188). There was no difference between the two cohorts in age, FIGO stage, grade, tumor residual, lymphatic invasion, subdivision and chemotherapy (Table 1). The flow chart of this study was presented in Figure 1A.

Identification of Prognostic PRLs in OC Patients

Firstly, we compared the expression of the 33 PRGs between OC tissues and normal ovary tissues using the TCGA datasets and GTEx datasets. The results suggested that 31 among 33 PRGs were either upregulated or downregulated in OC, compared to normal ovarian tissues (Figure 1B). Based on the lncRNA annotation file from the GENCODE website, we identified 14826 lncRNAs in the TCGA-RNA-seq dataset. To extract the potential PRLs, Pearson correlation analysis was performed to assess the correlation between PRGs and lncRNAs. Consequently, we obtained 2792 PRLs in the TCGA-RNA-seq dataset (Supplement Table 2). To assess the prognostic value of PRLs, univariate Cox regression analysis was performed, and 32 PRLs were identified to be notably associated with prognosis (Figure 1C). Besides, the Cytoscape software (3.8.2) was applied to briefly display the interactive relationships between prognostic PRLs and PRGs (Figure 1D).

Construction and Validation of the Prognostic PRLs Signature

To establish an optimal prognostic signature for predicting clinical outcome in OC patients, the LASSO-COX regression analysis was performed to screen out the most robust model from the candidate lncRNAs (Figure 2A and B). In summary,

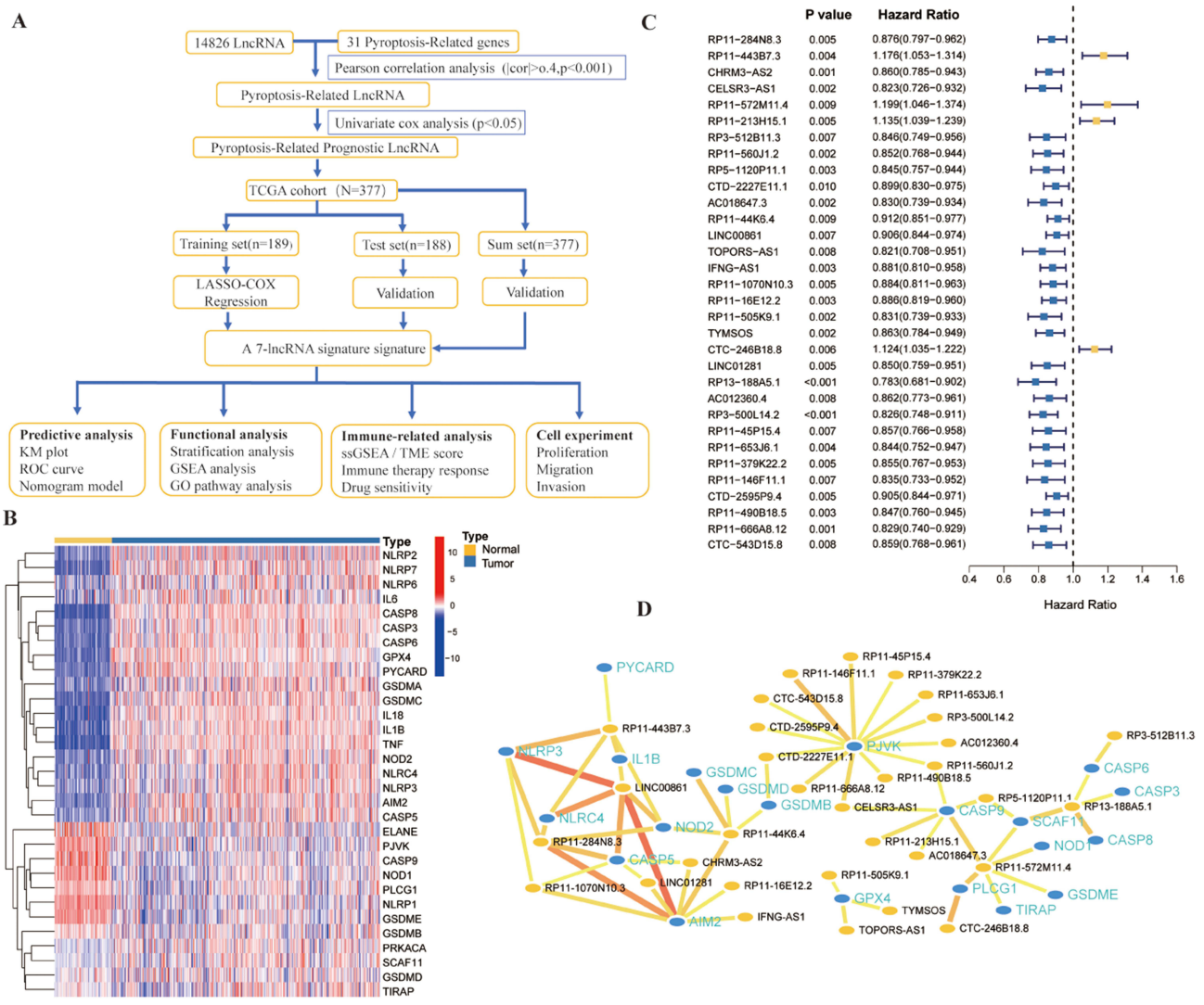

Figure 1 Identification of pyroptosis-related genes (PRGs) and pyroptosis-related lncRNAs (RPLs); (**A**) The flowchart of the whole process of data analysis; (**B**) A Heatmap of the PRGs between the normal ovary and tumor tissues (blue: low expression level; red: high expression level; Normal: brilliant blue; Tumor, yellow); (**C**) A forest plot of the prognostic ability of the PRLs; (**D**) The interaction network of the prognostic-PRLs and the PRGs (blue: PRGs; Orange: prognostic-PRLs).

we constructed a 7-PRLs prognostic signature and the risk score for each patient was assigned based on the coefficients of each lncRNA in the TCGA cohort (Figure 2C). The following is the formula for calculating the risk score: The risk score = (0.1506) * RP11-443B7.3 + (−0.1965) * CELSR3-AS1 + (0.1693) * RP11-213H15.1 + (−0.1342) * IFNG-AS1 + (−0.3121) * AC018647.3+ (0.2218) * CTC-246B18.8 + (−0.3302) * AC012360.4. Patients were divided into high- and low-risk subgroups depending on the best cutoff of risk score. Kaplan–Meier survival curves exhibited that the OS of patients with lower risk was substantially longer than those with high risk both in the training cohort and validation cohorts (test and sum cohort) (Figure 2D–F). Moreover, the time-dependent ROC curve analysis was carried out and the AUC value demonstrated that the signature harbored a promising ability to predict the 3-year OS and the 5-year OS, and the prognostic values of the signature in two validation cohorts were consistent with the findings in the training cohort (Figure 2G–I). The distributions of the risk score and survival status were listed in Figure 3A–F. It suggested that the risk score was associated with survival status. Furthermore, the different expressions of all the seven lncRNAs in the high- and low-risk subgroups were shown in the heatmap. The four protective lncRNAs (AC018647.3, AC012360.4, CELSR3-AS1, and IFNG-AS1) exhibited low expression in the high-risk subgroup; meanwhile, the other three risk lncRNAs (RP11-443B7.3, RP11-

 https://doi.org/10.2147/OTT.S491130

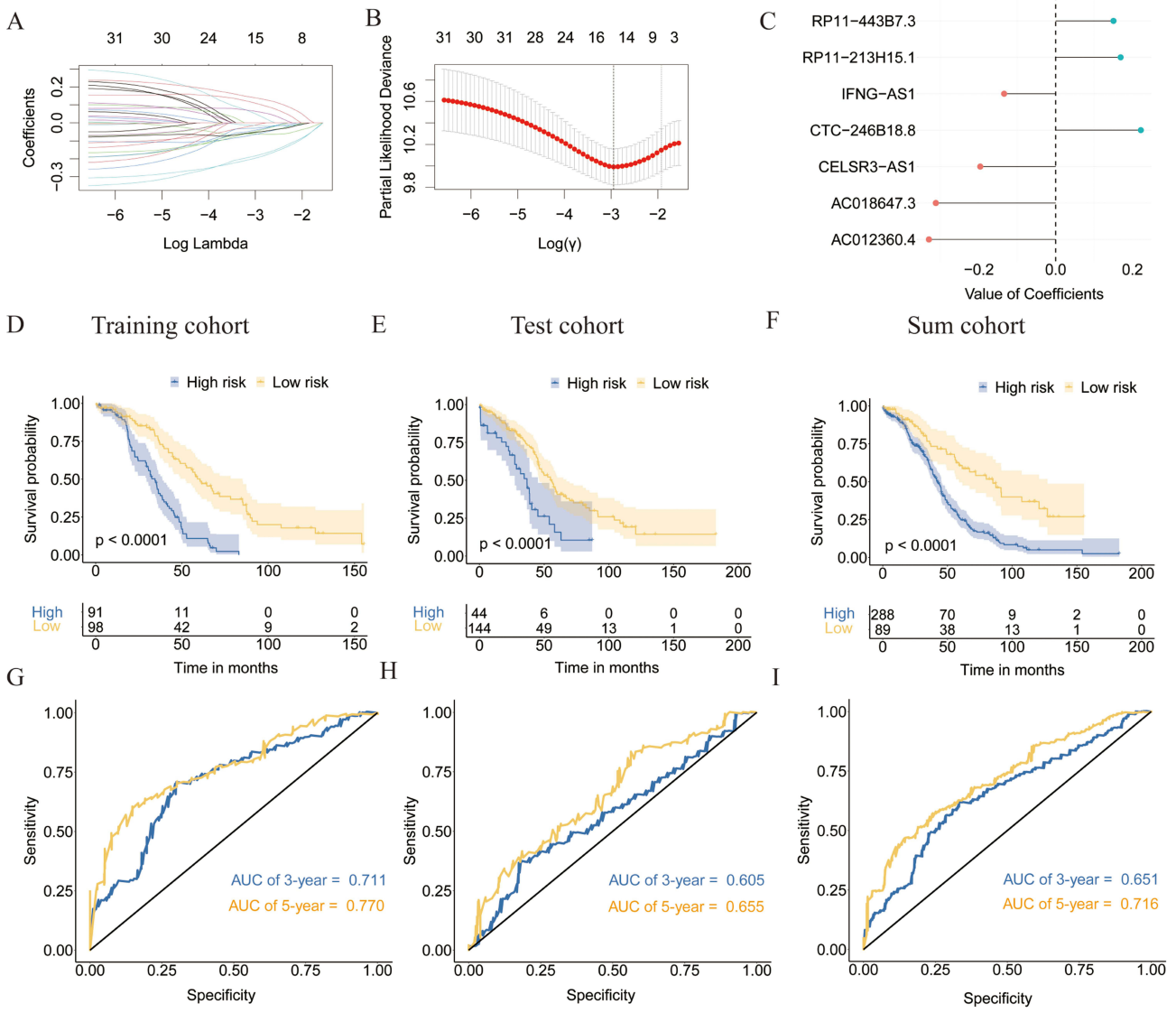

Figure 2 The construction and validation of a 7-PRLs prognostic signature. (**A**) LASSO regression of the prognostic PRLs; (**B**) 10 times cross-validation for tuning the parameter selection in the LASSO regression; (**C**) The coefficients of the signature; (**D–F**) Kaplan–Meier curves for the OS of patients in the training cohort (**D**) and the test cohort (**E**) and the sum cohort (**F**); (**G–I**) The time-dependent ROC curves to assess the prognostic capabilities of the risk score in the training cohort (**G**) and the test cohort (**H**) and the sum cohort (**I**).

213H15.1, and CTC-246B18.8) had high expression in the high-risk subgroup (Figure 3G–I). All these demonstrated that the 7-PRLs prognostic signature might solidly predict the clinical outcome of patients with OC.

Stratification Analysis of the Prognostic PRLs Signature

To better evaluate the prediction ability of the prognostic PRLs signature, the stratification analysis was subsequently performed. Compared to patients with high risk, patients with low risk had better OS in patients aged ≤55 and aged >55 subgroup (Figure 4A, $P = 0.00014$, $P < 0.0001$, respectively). Likewise, the prognostic PRLs signature retained its prognostic ability to predict OS for patients in advanced-stage subgroup (Figure 4B, $P < 0.0001$), low-grade subgroup (Figure 4C, $P = 0.0032$), high-grade subgroup (Figure 4C, $P < 0.0001$), lymphatic invasion subgroup (Figure 4D, $P = 0.048$), no lymphatic invasion subgroup (Figure 4D, $P = 0.0026$), no macroscopic disease subgroup (Figure 4E, $P = 0.0045$), 1–10 mm tumor residual subgroup (Figure 4E, $P = 0.00022$) and 20+ mm tumor residual subgroup (Figure 4E, $P = 0.00044$). Due to the small sample size, there was no remarkable difference in OS between high-risk patients and low-risk patients in early-stage subgroup (Figure 4B, $P = 0.19$) and 11–20 mm tumor residual subgroup (Figure 4E, $P = 0.078$). However, patients with high-

https://doi.org/10.2147/OTT.S491130

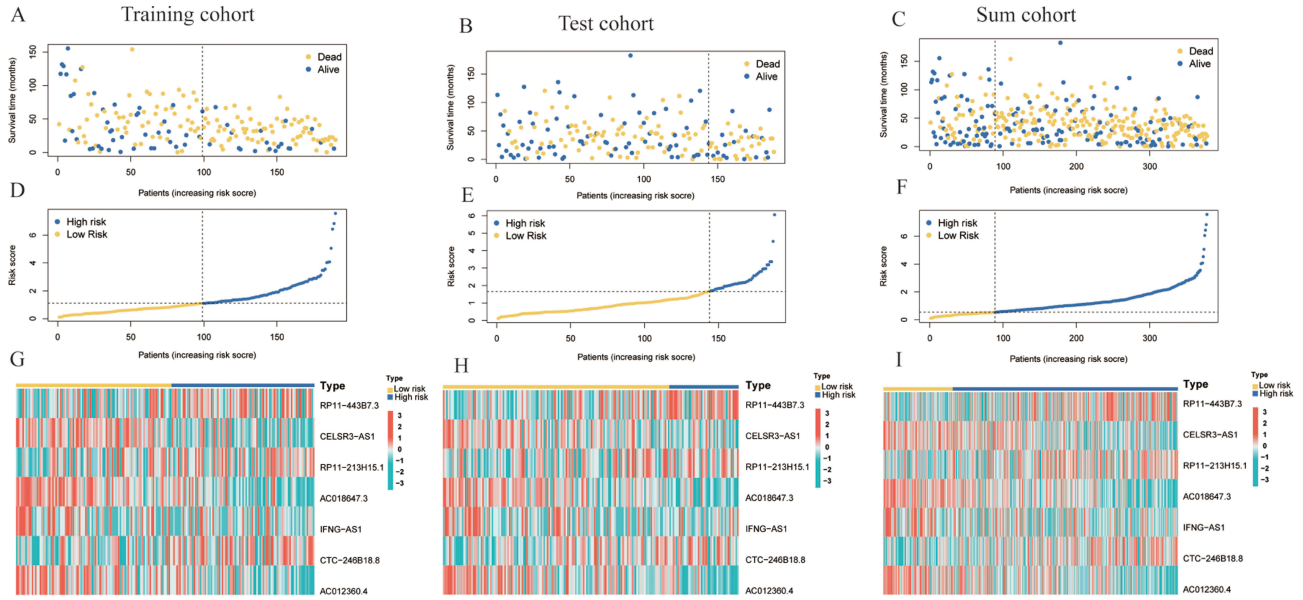

Figure 3 The association between risk score and survival status and seven PRLs expression; (**A–C**) The distributions of survival status of OC patients in the training cohort and the test cohort and the sum cohort; (**D–F**) The risk score calculated in the training cohort and the test cohort and the sum cohort; (**G–I**) The Heatmap showed the expression profiles of seven PRLs between the high- and low-risk subgroups.

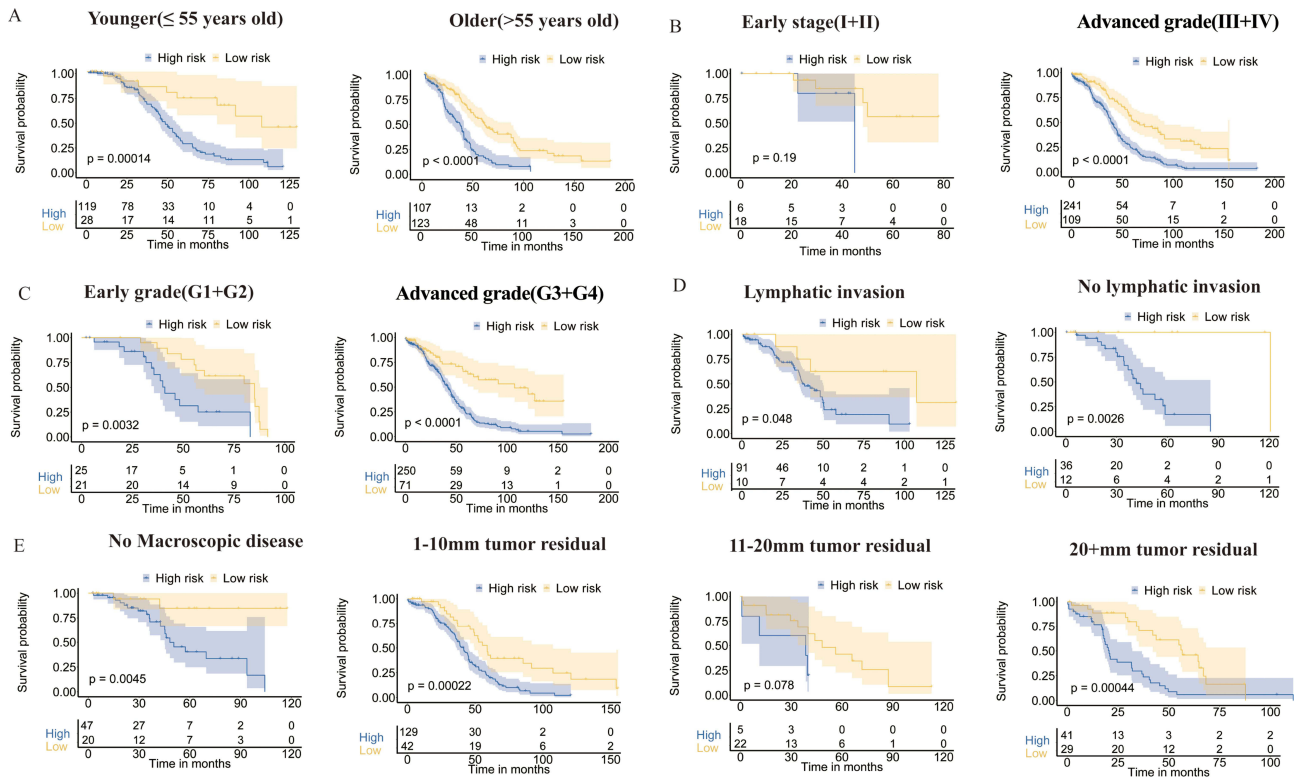

Figure 4 Stratification analysis to assess the prognostic value of risk score in subgroups divided based on age (**A**), FIGO stage (**B**), grade (**C**), lymphatic invasion (**D**) and tumor residual size (**E**).

risk score in these subgroups had the tendency for worse OS, in contrast to patients with low-risk. Altogether, these results suggested that the 7-PRLs prognostic signature retained its ability to predict OS in various subgroups and could serve as a potential predictor for OC patients.

https://doi.org/10.2147/OTT.S491130

Modeling the Prognostic Nomogram

In addition, Univariate and Multivariate Cox regression analysis were used to assess whether the prognostic PRLs signature was an independent prognostic factor. As shown in the forest plot, the red color presented the risk factors (HR > 1) and the blue one indicated the protective factors (HR < 1). The risk score (HR: 1.555; 95% CI: 1.391–1.739; $P < 0.001$), age (HR: 1.022; 95% CI: 1.009–1.035; $P < 0.001$), FIGO stage (HR: 1.395; 95% CI: 1.045–1.863; $P = 0.024$) but not grade (HR: 1.236; 95% CI: 0.842–1.814; $P = 0.279$) were associated with OS of patients (Figure 5A). Multivariate Cox analysis further proved that risk score (HR: 1.529; 95% CI: 1.367–1.709; $P < 0.001$), age (HR: 1.020; 95% CI: 1.008–1.032; $P = 0.001$), FIGO stage (HR: 1.401; 95% CI: 1.044–1.881; $P = 0.025$) but not grade (HR: 1.100; 95% CI: 0.741–1.631; $P = 0.636$) were independent prognostic factors for OC patients (Figure 5B). Thus, Age, FIGO stage and risk score were applied in the construction of a nomogram model (Figure 5C). Calibration plots indicated that the actual vs predicted rates of 3- and 5-year OS showed perfect concordance (Figure 5D). The diagram verified that the nomogram has a reliable and robust ability to predict the prognosis for OC patients.

Identification of the Biological Function of Prognostic PRLs Signature in OC

Gene Set Enrichment Analysis (GSEA) was employed to find the key pathways and biological functions that differ in the high- and low-risk subgroups. Firstly, $|\log FC| > 2$, $P < 0.05$ was identified as DEGs (Figure 6A). GSEA results suggested that the DEGs were mainly enriched in the inflammatory response pathway, p53 pathway, TGF-β signaling and TNFα signaling via NF-kB and so on (Figure 6B). Then, KEGG analysis and GO analysis were conducted and the outcomes displayed that the DEGs were mainly enriched in cell adhesion molecules, MAPK signaling pathway, NF-kB signaling pathway, PI3K-AKT signaling pathway, Wnt signaling pathway, primary immunodeficiency, and plentiful immune-related biological process (Figure 6C and D). Thus, these results suggested the PRLs may participate in the above pathways.

Association Between PRLs Signature and Immune Infiltration

Considering the enrichment analysis and the significant association between pyroptosis and immune status, we explored the relationship between risk score and tumor microenvironment infiltration. To explain the immune cell and stromal cell infiltration situation, we calculated the ESTIMATEScore, ImmuneScore, PurityScore and StromalScore. The correlation analysis implied that the risk score was positively relevant with the ESTIMATEScore (Figure 7A, r = 0.14, $P = 0.006$), and StromalScore (Figure 7C, r = 0.20, $P = 9.64e\text{-}05$) but negatively correlated with the PurityScore (Figure 7D, r = −0.14, $P = 0.005$). There was no correlation between risk score and ImmuneScore (Figure 7B, r = 0.215, $P = 0.06$). After that, the distribution proportion of different subpopulations of adaptive immunity cells and innate immunity cells in high- and low-risk subgroups were analyzed using the ssGSEA method. The distribution proportion of MHC class I cells and Type I IFN response was significantly lower in the high-risk subgroup than the low-risk subgroup (Figure 7E). In addition, the potential response of individual patients to immunotherapy was appraised using the TIDE algorithm. Our results showed that patients with low-risk score were potentially more sensitive to immunotherapy than patients with high-risk score (Figure 7F), which might be associated with higher expression of PD-L1, CTAL4 and LAG3 in low-risk group (Figure 7G–I). Taken together, we speculated that patients with high-risk score might recruit multiple immune cells and stromal cells and escape immune surveillance. Due that the predominant therapeutics for OC patients were still chemotherapy, we contrasted the sensitivity to a variety of anticancer drugs between the high- and low-risk subgroups (Supplement Table 3). The results displayed that the IC50s of veliparib and metformin were higher in patients with higher risk score, which means the shrinkage risk occurs with the growing sensitivity to veliparib and metformin (Figure 8). Unfortunately, there was no significant difference in IC50 of cisplatin and paclitaxel between two subgroups (Supplement Figure 1). All this evidence indicated that veliparib and metformin might be a good choice for OC patients with low-risk score.

Inhibition of LncRNA TYMSOS Reduced Cell Proliferation, Invasion and Migration

Due to the high abundance, TYMSOS was further validated in SKOV3 and A2780 ovarian cancer cell lines. Firstly, we analyzed the different expression of TYMOS in normal ovary tissues and OC tissues. The results showed that TYMSOS expression was significantly upregulated in tumor tissues, compared to normal ovary tissues (Figure 9A). In contrast to

https://doi.org/10.2147/OTT.S491130

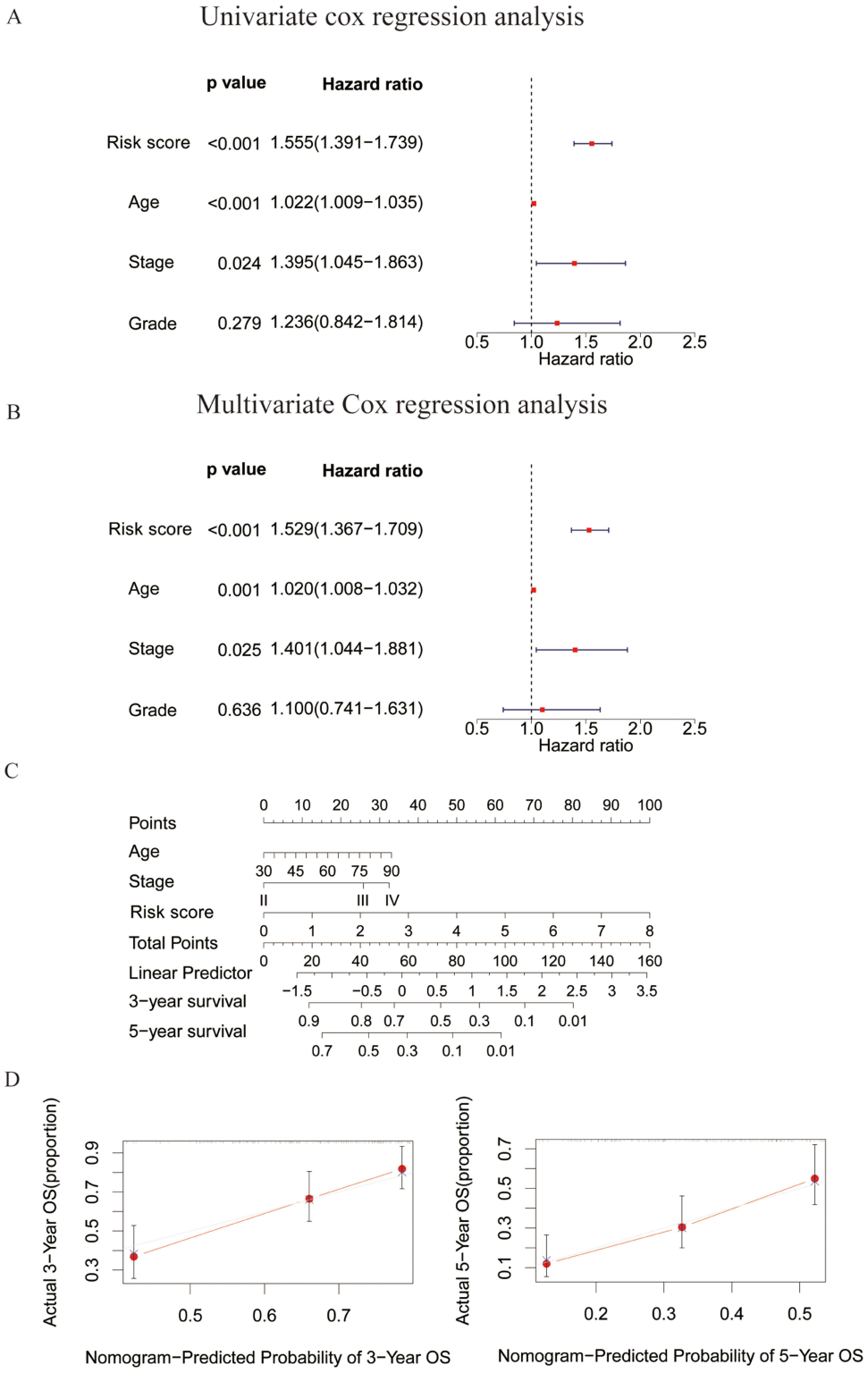

Figure 5 Construction of nomogram based on clinical features and risk score. (**A** and **B**) The forest plot represents the univariate and multivariate Cox analyses to select the independent prognostic predictors; (**C**) Establishment of a nomogram based on risk score, age, and stage to predict 3-, 5-year OS in the TCGA cohort; (**D**) Calibration plots of the nomogram to predict OS at 3-, 5-year.

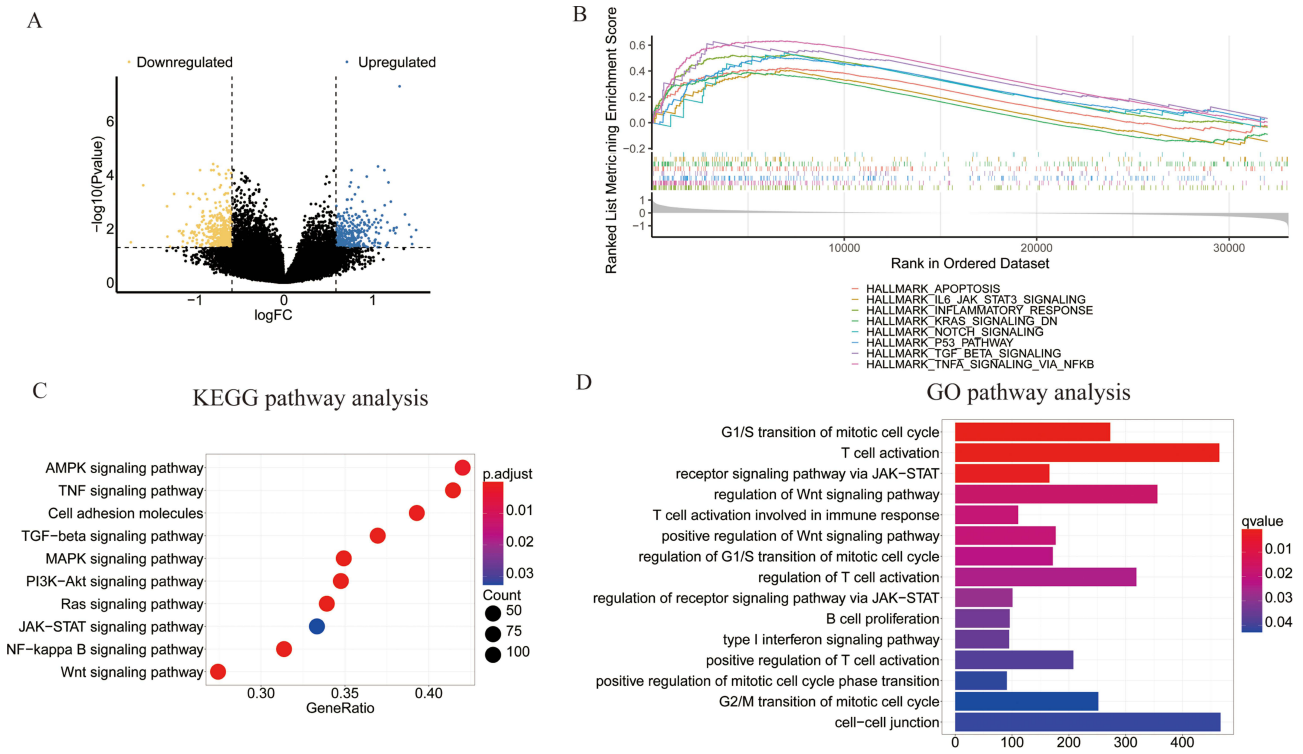

Figure 6 Functional analysis based on the DEGs between the high- and low-risk subgroups. (**A**) The volcano plot showed the different expression genes between high- and low-risk subgroups; (**B**) Gene set enrichment analysis to screen DEGs; (**C**) The bubble plot displayed the analysis of KEGG pathway enrichment; (**D**) The bar plot revealed the analysis of GO pathway enrichment.

patients with low expression of TYMSOS, patients with high expression of TYMSOS had worse OS in GSE26193 dataset (Figure 9B). To reveal the role of TYMSOS in OC, the endogenous expression of TYMSOS in SKOV3 and A2780 cells was interfered with siRNA (Figure 9C). CCK-8 assay indicated that the inhibition of TYMSOS decreased cell proliferation (Figure 9D and E). In addition, inhibition of TYMSOS apparently reduced the migration and invasion ability of OC cells (Figure 9F and G). It has been reported that overexpression of GSDMD and GPX4 defect induced pyroptosis, and we found that TYMSOS was positively correlated with the expression of GPX4 (Figure 9H, r = 0.48, P = 8.1e-31) and negatively correlated with the expression of GSDMD (Figure 9H, r=−0.26, P = 4.2e-9) in TCGA-GETx combined datasets. More importantly, TYMSOS inhibition significantly increased the expression of GSDMD and decreased the mRNA expression of GPX4 (Figure 9I). All these indicated that inhibition of lncRNA TYMSOS reduced cell proliferation, invasion and migration via promoting pyroptosis.

Discussion

OC is one of the most common gynecologic malignancies with a high mortality rate in the world. Consequently, there is of great importance to identify reliable and effective biomarkers for the OC prognosis. In prior research, the lncRNA signatures for prognostic prediction have been validated in many categories of cancers,[38] and there is even a database Lnc2Cancer 3.0, which includes comprehensive data on experimentally supported long non-coding RNAs (lncRNAs) and circular RNAs (circRNAs) associated with human cancers.[39] In the same way, based on the differentially expressed lncRNAs and illness etiology, several lncRNA-associated signatures have correspondingly been constructed to forecast the outcome of OC patients.[40,41] Nevertheless, the mutual interactions of PRLs in prognosis of OC patients remain unclear. In this study, we reported a prognostic PRLs signature, providing a promising strategy for prognosis and immune features in OC patient, which have important clinical implications for guiding individual treatment and improving the effectiveness of the immune response. Taking advantage of the TCGA and GTEx databases, we compared the mRNA expression of 33 PRGs in OC samples and normal ovary tissues. Surprisingly, we discovered that all PRGs except two genes (CASP1 and

https://doi.org/10.2147/OTT.S491130

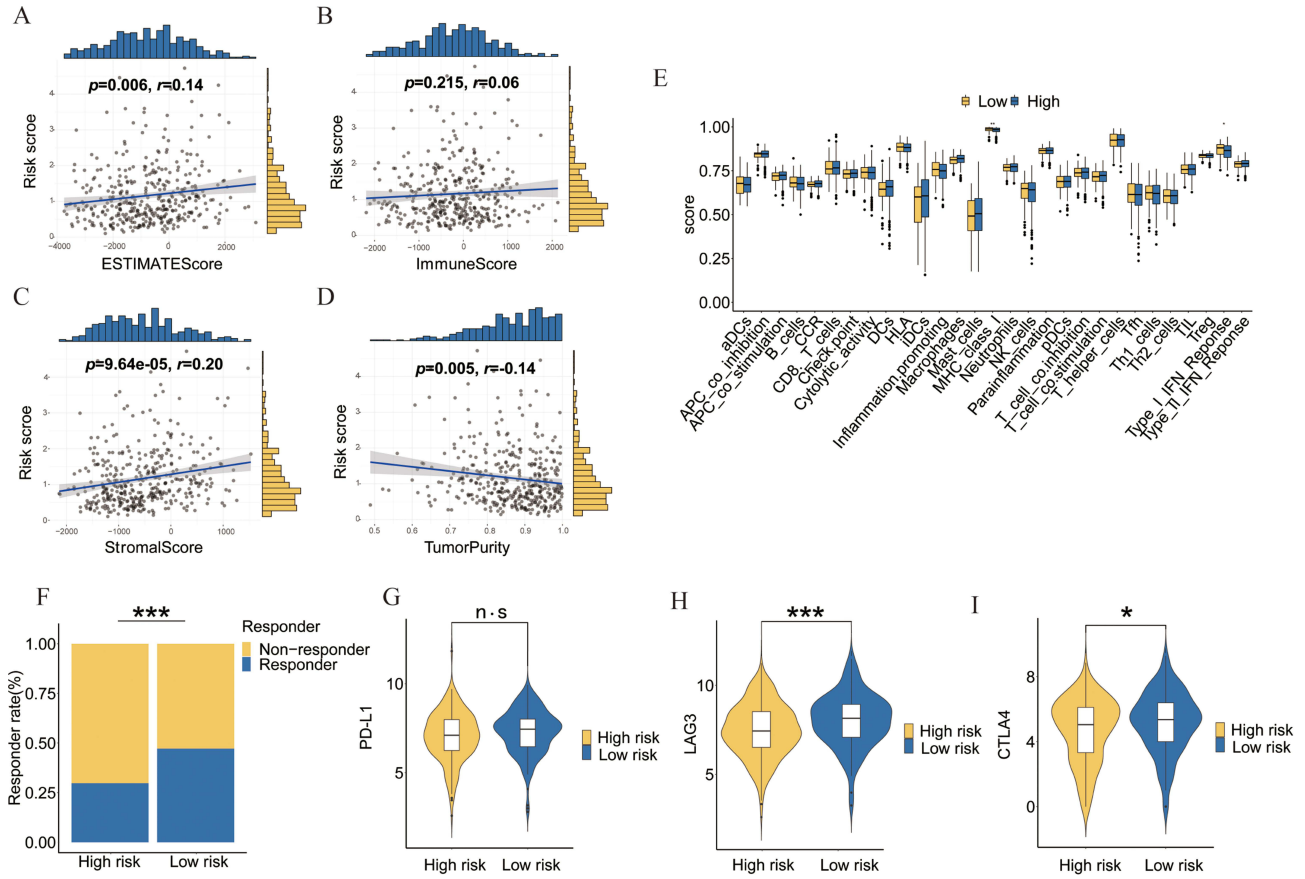

Figure 7 Association between the prognostic PRLs signature and tumor microenvironment infiltration and immunotherapy response. (**A**–**D**) Correlation between risk score and ESTIMATEScore, ImmuneScore, StromalScore and TumorPurity; (**E**) The differences of immune cells calculated by the ssGSEA analysis in high- and low-risk subgroups; (**F**) The different proportion of patients between high- and low-risk subgroups to immunotherapy; (**G**–**I**) The different expression of immune checkpoints including PD-L1, CTLA4 and LAG3 in high- and low-risk subgroups. *P < 0.05, ***P < 0.001, ****P < 0.0001; n.s indicates non-significant.

CASP4) were differently expressed in tumor samples. Subsequently, 32 lncRNAs associated with OS were picked out and defined as prognostic PRLs. Unexpectedly, several prognostic PRLs have been identified to play important roles in various cancers. For instance, Overexpression of TOPORS-AS1 was supposed to inhibit ovarian cancer cell proliferation and restrain cell aggressive behavior in vivo and in vitro.[42] LINC01281 was confirmed as immune-associated lncRNAs for predicting prognosis in cervical cancer.[43] Subsequently, we performed LASSO-COX regression to construct a 7-PRLs prognostic signature. The KM plotter analysis and AUC curves suggested that the prognostic PRLs signature might effectively predict the clinical outcome of OC patients. Furthermore, stratification analysis indicated that the prognostic PRLs signature still retained its prognostic ability to predict OS for patients without considering other clinical features. Multivariate Cox regression analysis showed that risk score was an independent risk factor for prognosis of OC patients. For better clinical applicability of the signature, we also created a nomogram. GSEA analysis was then carried out to explore the potential functions of the PRLs. The results demonstrated that the PRLs had a robust association with cell proliferation and immunity. It's worth mentioning that GSDME expression has been reported to enhance both the number and functions of tumor-infiltrating natural killer and CD8+ T lymphocytes to increase the phagocytosis of tumor cells.[44] Natural killer cells and cytotoxic T lymphocytes kill gasdermin B (GSDMB)-positive cells through pyroptosis.[45] In addition, several lncRNAs were also validated to participate in immune pathways through the process of pyroptosis.[46] Therefore, we then analyzed the different distributions of immune function and immune cells between high- and low-risk subgroups. Our results indicated that the risk score was associated with tumor microenvironment infiltration and immune response. Various immune cells, especially MHC class I cells and Type I IFN response, were differently distributed in the high-risk group and low-risk group. All the evidence revealed that patients with high-risk score might recruit multiple

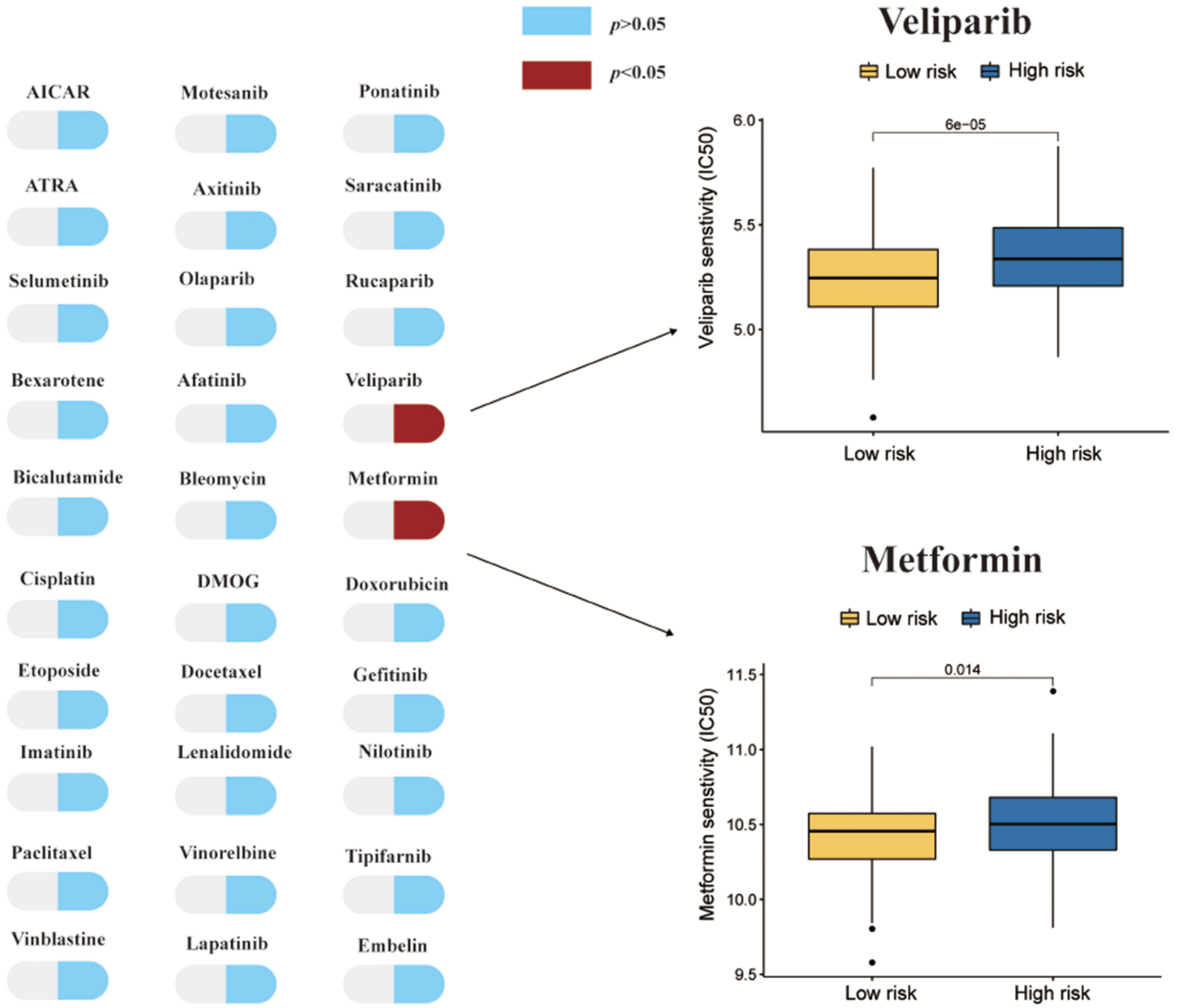

Figure 8 Estimated drug sensitivity in patients with high- and low-risk subgroups.

immune cells and stromal cells and escape immune surveillance. Also, we conducted a comparison of the sensitivity of 138 common anti-cancer drugs between the high-risk and low-risk groups. It suggested that patients with high risk acquired drug-resistance in metformin and veliparib, which acted as the first-line Chemotherapy and Maintenance Therapy in OC.[47] Finally, the expressive abundance of several lncRNAs in ovarian cancer cell lines were detected (Data not shown). Due to the high abundance, TYMSOS was selected for further validation. TYMSOS inhibition significantly decreased the cell proliferation, invasion and migration in A2780 and SKOV3 ovarian cancer cell lines. Inhibition of TYMSOS increased the expression of GSDMD and decreased the expression of GPX4. Besides, TYMSOS was highly expressed in ovarian cancer tissues, and high expression of TYMSOS was associated with worse OS in GSE26193 dataset. All these evidences proved that TYMSOS might regulate cell proliferation and aggressive behavior through pyroptosis pathway and it might serve as a novel target to treat OC patients.

Recently, several PRLs signature in OC have been constructed.[48–51] Compared with the reported risk signatures, our risk signature has the higher prediction prognostic ability with the 5-year AUC = 0.770 in training cohort and 5-year AUC = 0.716 in sum cohort. Obviously, there are lots of limitations in our study. Firstly, the biggest limitation is that external validation datasets are lacking, which makes the results less credible. Secondly, the mechanisms of PRLs in OC are only predicted by using online datasets and that is insufficient. In addition, whether the PRLs identified in our study can regulate prognosis of OC

https://doi.org/10.2147/OTT.S491130

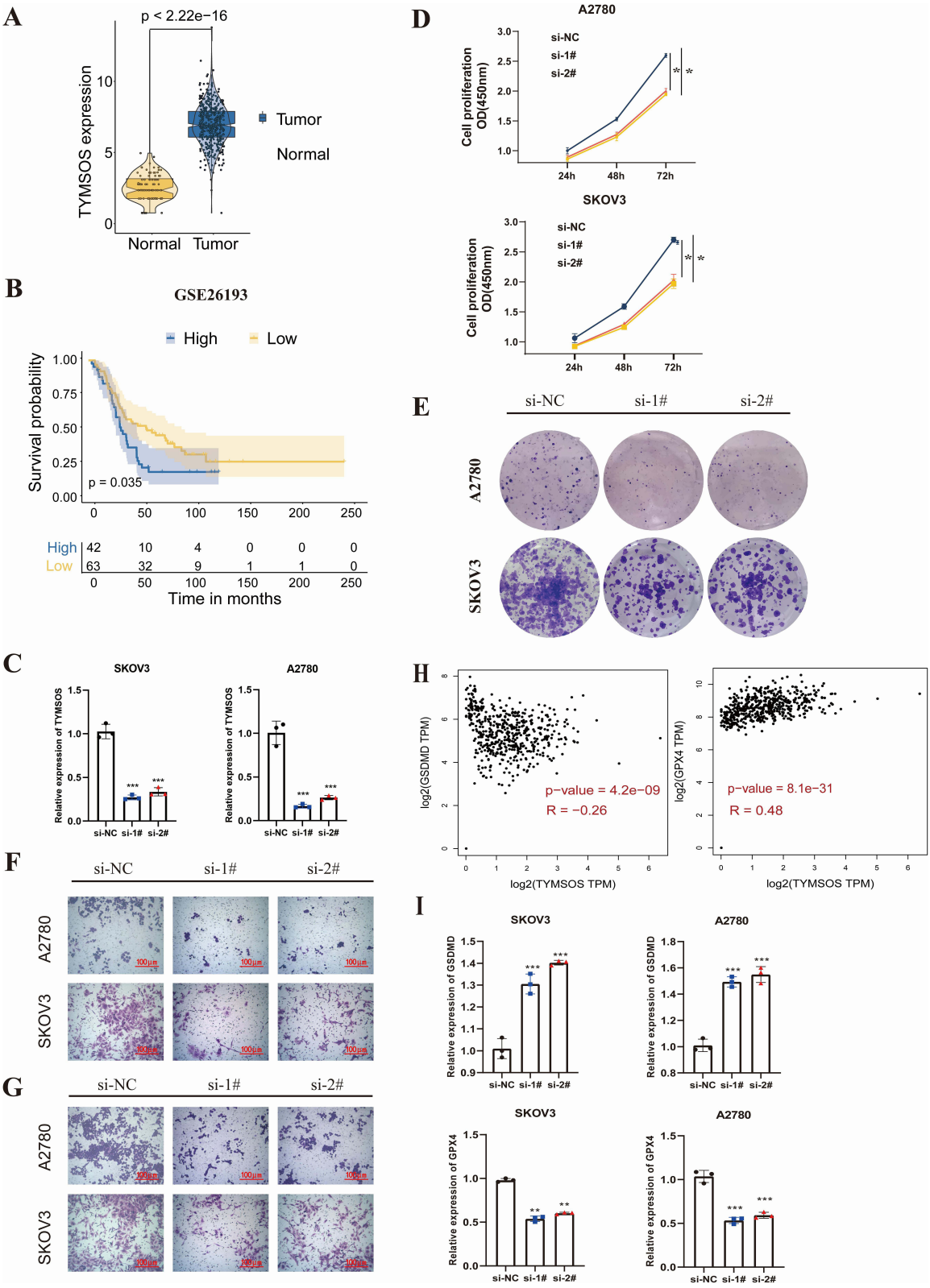

Figure 9 Inhibition of lncRNA TYMSOS reduced cell proliferation, invasion and migration. (**A**) TYMSOS was significantly upregulated in ovarian cancer tissues; (**B**) The KM plot showed that the high expression of TYMSOS had a remarkably worse prognosis in GSE26193 cohorts; (**C**) The expression of TYMSOS was significantly inhibited after treating with siRNA for 48h. (**D** and **E**) the inhibition of TYMSOS significantly reduced the proliferation of A2780 and SKOV3 cells; (**F** and **G**) Inhibition of TYMSOS led to remarkable decrease in migratory capacity and invasion ability of A2780 and SKOV3 cells; (**H**) TYMSOS was negatively correlated with GSDMD and positively correlated with GPX4 in the TCGA and GTEx combined dataset; (**I**) Inhibition of TYMSOS expression increased the mRNA expression of GSDMD and decreased the mRNA expression of GPX4 in A780 and SKOV3 cell lines. **P* < 0.05, ***P* < 0.01, ****P* < 0.001.

patients is not validated in our self-test samples. Finally, the effect of TYMSOS on clinical outcome and pyroptosis in OC is also inadequate. Therefore, further experimental research should be performed in the future.

Conclusions

In conclusion, our study constructed a novel prognostic signature based on PRLs in silico. It effectively predicted the clinical outcome of OC patients. Except to prognosis, the tumor microenvironment infiltration, immune response and drug sensitivity were potentially different in high- and low-risk subgroups.

Data Sharing Statement

All analyzed data are included in this published article and its supplementary information file. The datasets used and/or analyzed during the current study are available from the corresponding author on reasonable request.

Ethics Approval and Consent to Participate

The study was approved by the Institutional Review Board of Hunan Cancer Hospital.

Acknowledgments

We acknowledge TCGA and GEO databases for providing their platforms and contributors for uploading their meaningful datasets. This paper has been uploaded to Preprints.org as a preprint: https://www.preprints.org/manuscript/202201.0346/v1.

Author Contributions

All authors made a significant contribution to the work reported, whether that is in the conception, study design, execution, acquisition of data, analysis and interpretation, or in all these areas; took part in drafting, revising or critically reviewing the article; gave final approval of the version to be published; have agreed on the journal to which the article has been submitted; and agree to be accountable for all aspects of the work.

Funding

This research was supported by the Young Scientists Fund of the National Natural Science Foundation of China (NO.82303035), the Natural Science Foundation of Hunan Province (2024JJ5245, 2024JJ9268), Scientific Research Project of Hunan Provincial Health Commission (202314017963), the Youth Natural Science Foundation of Hunan Province (2022JJ40252).

Disclosure

The authors declare that there are no conflicts of interest.

References

1. Menon U, Karpinskyj C, Gentry-Maharaj A. Ovarian cancer prevention and screening. *Obstet Gynecol*. 2018;131(5):909–927. doi:10.1097/AOG.0000000000002580
2. Siegel RL, Giaquinto AN, Jemal A. Cancer statistics, 2024 [published correction appears in CA Cancer J Clin. 2024 Mar-Apr;74(2):203]. *CA Cancer J Clin*. 2024;74(1):12–49. doi:10.3322/caac.21820
3. Kuroki L, Guntupalli SR. Treatment of epithelial ovarian cancer. *BMJ*. 2020;371:m3773. doi:10.1136/bmj.m3773
4. Holmes D. The problem with platinum. *Nature*. 2015;527(7579):S218–S219. doi:10.1038/527S218a
5. Koren E, Fuchs Y. Modes of regulated cell death in cancer. *Cancer Discov*. 2021;11(2):245–265. doi:10.1158/2159-8290.CD-20-0789
6. Bergsbaken T, Fink SL, Cookson BT. Pyroptosis: host cell death and inflammation. *Nat Rev Microbiol*. 2009;7(2):99–109. doi:10.1038/nrmicro2070
7. Kovacs SB, Miao EA. Gasdermins: effectors of pyroptosis. *Trends Cell Biol*. 2017;27(9):673–684. doi:10.1016/j.tcb.2017.05.005
8. Shi J, Gao W, Shao F. Pyroptosis: gasdermin-mediated programmed necrotic cell death. *Trends Biochem Sci*. 2017;42(4):245–254. doi:10.1016/j.tibs.2016.10.004
9. Miao EA, Rajan JV, Aderem A. Caspase-1-induced pyroptotic cell death. *Immunol Rev*. 2011;243(1):206–214. doi:10.1111/j.1600-065X.2011.01044.x
10. Broz P, Pelegrín P, Shao F. The gasdermins, a protein family executing cell death and inflammation. *Nat Rev Immunol*. 2020;20(3):143–157. doi:10.1038/s41577-019-0228-2

11. Robinson N, Ganesan R, Hegedűs C, Kovács K, Kufer TA, Virág L. Programmed necrotic cell death of macrophages: focus on pyroptosis, necroptosis, and parthanatos. *Redox Biol*. 2019;26:101239. doi:10.1016/j.redox.2019.101239
12. Zhu Q, Zheng M, Balakrishnan A, Karki R, Kanneganti TD. Gasdermin D promotes AIM2 inflammasome activation and is required for host protection against *Francisella novicida*. *J Immunol*. 2018;201(12):3662–3668. doi:10.4049/jimmunol.1800788
13. Thurston TL, Matthews SA, Jennings E, et al. Growth inhibition of cytosolic Salmonella by caspase-1 and caspase-11 precedes host cell death. *Nat Commun*. 2016;7:13292. doi:10.1038/ncomms13292
14. Cerqueira DM, Gomes MTR, Silva ALN, et al. Guanylate-binding protein 5 licenses caspase-11 for Gasdermin-D mediated host resistance to Brucella abortus infection. *PLoS Pathog*. 2018;14(12):e1007519. doi:10.1371/journal.ppat.1007519
15. Xiao J, Wang C, Yao JC, et al. Gasdermin D mediates the pathogenesis of neonatal-onset multisystem inflammatory disease in mice. *PLoS Biol*. 2018;16(11):e3000047. doi:10.1371/journal.pbio.3000047
16. Kanneganti A, Malireddi RKS, Saavedra PHV, et al. GSDMD is critical for autoinflammatory pathology in a mouse model of familial Mediterranean fever. *J Exp Med*. 2018;215(6):1519–1529. doi:10.1084/jem.20172060
17. Grivennikov SI, Greten FR, Karin M. Immunity, inflammation, and cancer. *Cell*. 2010;140(6):883–899. doi:10.1016/j.cell.2010.01.025
18. Molina-Crespo Á, Cadete A, Sarrio D, et al. Intracellular delivery of an antibody targeting gasdermin-B reduces HER2 breast cancer aggressiveness. *Clin Cancer Res*. 2019;25(15):4846–4858. doi:10.1158/1078-0432.CCR-18-2381
19. Wang WJ, Chen D, Jiang MZ, et al. Downregulation of gasdermin D promotes gastric cancer proliferation by regulating cell cycle-related proteins. *J Dig Dis*. 2018;19(2):74–83. doi:10.1111/1751-2980.12576
20. Liu X, Xia S, Zhang Z, Wu H, Lieberman J. Channelling inflammation: gasdermins in physiology and disease. *Nat Rev Drug Discov*. 2021;20(5):384–405. doi:10.1038/s41573-021-00154-z
21. Statello L, Guo CJ, Chen LL, Huarte M. Gene regulation by long non-coding RNAs and its biological functions [published correction appears in Nat Rev Mol Cell Biol. 2021 Jan 8]. *Nat Rev mol Cell Biol*. 2021;22(2):96–118. doi:10.1038/s41580-020-00315-9
22. Ye Y, Dai Q, Qi H. A novel defined pyroptosis-related gene signature for predicting the prognosis of ovarian cancer. *Cell Death Discov*. 2021;7(1):71. doi:10.1038/s41420-021-00451-x
23. Li XY, Zhang LY, Li XY, Yang XT, Su LX. A pyroptosis-related gene signature for predicting survival in glioblastoma. *Front Oncol*. 2021;11:697198. doi:10.3389/fonc.2021.697198
24. Shao W, Yang Z, Fu Y, et al. The pyroptosis-related signature predicts prognosis and indicates immune microenvironment infiltration in gastric cancer. *Front Cell Dev Biol*. 2021;9:676485. doi:10.3389/fcell.2021.676485
25. Dong Z, Bian L, Wang M, Wang L, Wang Y. Identification of a pyroptosis-related gene signature for prediction of overall survival in lung adenocarcinoma. *J Oncol*. 2021;2021:6365459. doi:10.1155/2021/6365459
26. Liang H, Yu T, Han Y, et al. LncRNA PTAR promotes EMT and invasion-metastasis in serous ovarian cancer by competitively binding miR-101-3p to regulate ZEB1 expression [published correction appears in Mol Cancer. 2021 Apr 9;20(1):64]. *Mol Cancer*. 2018;17(1):119. doi:10.1186/s12943-018-0870-5
27. Lou W, Ding B, Zhong G, Du C, Fan W, Fu P. Dysregulation of pseudogene/lncRNA-hsa-miR-363-3p-SPOCK2 pathway fuels stage progression of ovarian cancer. *Aging*. 2019;11(23):11416–11439. doi:10.18632/aging.102538
28. Zhao H, Ding F, Zheng G. LncRNA TMPO-AS1 promotes LCN2 transcriptional activity and exerts oncogenic functions in ovarian cancer. *FASEB J*. 2020;34(9):11382–11394. doi:10.1096/fj.201902683R
29. Latz E, Xiao TS, Stutz A. Activation and regulation of the inflammasomes. *Nat Rev Immunol*. 2013;13(6):397–411. doi:10.1038/nri3452
30. Zhang X, Sun S, Pu JK, et al. Long non-coding RNA expression profiles predict clinical phenotypes in glioma. *Neurobiol Dis*. 2012;48(1):1–8. doi:10.1016/j.nbd.2012.06.004
31. Hong W, Liang L, Gu Y, et al. Immune-related lncRNA to construct novel signature and predict the immune landscape of human hepatocellular carcinoma. *Mol Ther Nucleic Acids*. 2020;22:937–947. doi:10.1016/j.omtn.2020.10.002
32. Goeman JJ. L1 penalized estimation in the Cox proportional hazards model. *Biom J*. 2010;52(1):70–84. doi:10.1002/bimj.200900028
33. Li H, Wu N, Liu ZY, Chen YC, Cheng Q, Wang J. Development of a novel transcription factors-related prognostic signature for serous ovarian cancer. *Sci Rep*. 2021;11(1):7207. doi:10.1038/s41598-021-86294-z
34. Yoshihara K, Shahmoradgoli M, Martínez E, et al. Inferring tumour purity and stromal and immune cell admixture from expression data. *Nat Commun*. 2013;4:2612. doi:10.1038/ncomms3612
35. Newman AM, Liu CL, Green MR, et al. Robust enumeration of cell subsets from tissue expression profiles. *Nat Methods*. 2015;12(5):453–457. doi:10.1038/nmeth.3337
36. Jiang P, Gu S, Pan D, et al. Signatures of T cell dysfunction and exclusion predict cancer immunotherapy response. *Nat Med*. 2018;24(10):1550–1558. doi:10.1038/s41591-018-0136-1
37. Nick TG, Hardin JM. Regression modeling strategies: an illustrative case study from medical rehabilitation outcomes research. *Am J Occup Ther*. 1999;53(5):459–470. doi:10.5014/ajot.53.5.459
38. Tan YT, Lin JF, Li T, Li JJ, Xu RH, Ju HQ. LncRNA-mediated posttranslational modifications and reprogramming of energy metabolism in cancer. *Cancer Commun*. 2021;41(2):109–120. doi:10.1002/cac2.12108
39. Gao Y, Shang S, Guo S, et al. Lnc2Cancer 3.0: an updated resource for experimentally supported lncRNA/circRNA cancer associations and web tools based on RNA-seq and scRNA-seq data. *Nucleic Acids Res*. 2021;49(D1):D1251–D1258. doi:10.1093/nar/gkaa1006
40. Yang H, Gao L, Zhang M, et al. Identification and analysis of an epigenetically regulated Five-lncRNA signature associated with outcome and chemotherapy response in ovarian cancer. *Front Cell Dev Biol*. 2021;9:644940. doi:10.3389/fcell.2021.644940
41. Zheng M, Hu Y, Gou R, et al. Identification three LncRNA prognostic signature of ovarian cancer based on genome-wide copy number variation. *Biomed Pharmacother*. 2020;124:109810. doi:10.1016/j.biopha.2019.109810
42. Fu Y, Katsaros D, Biglia N, et al. Vitamin D receptor upregulates lncRNA TOPORS-AS1 which inhibits the Wnt/β-catenin pathway and associates with favorable prognosis of ovarian cancer. *Sci Rep*. 2021;11(1):7484. doi:10.1038/s41598-021-86923-7
43. Ye J, Chen X, Lu W. Identification and experimental validation of immune-associate lncRNAs for predicting prognosis in cervical cancer. *Onco Targets Ther*. 2021;14:4721–4734. doi:10.2147/OTT.S322998
44. Zhang Z, Zhang Y, Xia S, et al. Gasdermin E suppresses tumour growth by activating anti-tumour immunity. *Nature*. 2020;579(7799):415–420. doi:10.1038/s41586-020-2071-9

45. Zhou Z, He H, Wang K, et al. Granzyme A from cytotoxic lymphocytes cleaves GSDMB to trigger pyroptosis in target cells. *Science*. 2020;368 (6494):eaaz7548. doi:10.1126/science.aaz7548
46. Wan P, Su W, Zhang Y, et al. LncRNA H19 initiates microglial pyroptosis and neuronal death in retinal ischemia/reperfusion injury [published correction appears in Cell Death Differ. 2023 Mar;30(3):859]. *Cell Death Differ*. 2020;27(1):176–191. doi:10.1038/s41418-019-0351-4
47. Coleman RL, Fleming GF, Brady MF, et al. Veliparib with first-line chemotherapy and as maintenance therapy in ovarian cancer. *N Engl J Med*. 2019;381(25):2403–2415. doi:10.1056/NEJMoa1909707
48. Zhang ZY, Xu ZJ, Yan YL. Role of a pyroptosis-related lncRNA signature in risk stratification and immunotherapy of ovarian cancer. *Front Med*. 2022;8:93515. doi:10.3389/fmed.2021.793515
49. Wu YL, Liang L, Li Q, et al. The role of pyroptosis-related lncRNA risk signature in ovarian cancer prognosis and immune system. *Discov Oncol*. 2023;14(1):149. doi:10.1007/s12672-023-00767-3
50. Xu HY, Lu M, Liu YN, et al. Identification of a pyroptosis-related long non-coding RNA signature for prognosis and its related ceRNA regulatory network of ovarian cancer. *J Cancer*. 2023;14(16):3151–3168. doi:10.7150/jca.88485
51. Cao XY, Zhang QQ, Zhu Y, et al. Derivation, comprehensive analysis, and assay validation of a pyroptosis-related lncRNA prognostic signature in patients with ovarian cancer. *Front Oncol*. 2022;12:780950. doi:10.3389/fonc.2022.780950